Experimental investigation on environmental control of a 50-person mine refuge chamber

Zujing Zhang[a*], Ting Jin[a], Hongwei Wu[b], Rodney Day[b], Xiangkui Gao[c], Kequan Wang[d], Ruiyong Mao[a**]

[a] College of Civil Engineering, Guizhou University, Guiyang, 550025, China
[b] School of Physics, Engineering and Computer Science, University of Hertfordshire, Hatfield, AL10 9AB, United Kingdom
[c] State Key Laboratory for GeoMechanics and Deep Underground Engineering, Xuzhou, Jiangsu 221116, China
[d] State Key Laboratory of the Gas Disaster Detecting, Preventing and Emergency Controlling, China Coal Technology and Engineering Group Chongqing Research Institute, Chongqing 400037, China

[*]Corresponding author: tel: +86 185 2391 9513, email: zjzhang3@gzu.edu.cn.
[**]Corresponding author: tel: +86 139 8505 6628, email: rymao@gzu.edu.cn.

Abstract

Air quality and thermal environment of mine refuge chamber (MRC) are very important to determine the physical safety of refugees. Accurately assessing the environmental load and taking reasonable measures are critical to achieve the environmental control goals of MRC. In order to evaluate the metabolic parameters of occupants and the effectiveness of environmental control measures in a MRC, in this research, 50 adult men entered a MRC laboratory for an 8-hour test. During the test, the compressed O_2 cylinders and air purification devices were used to ensure the indoor air quality. The possibility of using chemical adsorbents to passively scrub CO_2 and the performance of dehumidification by mine compressed air (MCA) were also investigated by simulation experiments. The results indicated that: (1) The per capita metabolic rates of O_2, CO_2 and heat during the refuge process are 0.34~0.37 L/min, 0.34 L/min and 117~128 W, respectively. (2) When $Ca(OH)_2$ particles are used as CO_2 adsorbent, the air purification device has both dehumidification and CO_2 scrubbing functions, and three air purification devices could make the CO_2 concentration below 0.8% with the relative humidity below 76%. When $Ca(OH)_2$ particles are packaged to passively scrub CO_2, the amount of adsorbent may increase significantly. (3) When MCA is used for dehumidification in a MRC, the air volume of 0.15 m^3/min per capita could maintain the relative humidity close to 60%. (4) In the early stage of disaster avoidance, the indoor ambient temperature rises rapidly within 1 h followed by a slight increase.

Keywords: Mine refuge chamber; human metabolic rate; air quality; ambient temperature; relative humidity

1 Introduction

With the increase of energy resource consumption and demand, the depth of commercial exploitation of mines worldwide has also been increasing (Dou *et al.*, 2020). In China, by the end of 2020, there are about 4,700 coal mines and 32,000 non-coal mines. Potential accidents such as explosion, fire, collapse can make underground mining to be one of the most dangerous production activities (Onifade, 2021). Mine refuge chamber (MRC) is constructed in the underground surrounding rock along the roadway and relatively isolated from the roadway environment, which provides breathable air, water and supplies in the event of an emergency within 96 h when miners are unable to escape (Halim and Brune, 2019). MRC system has been adopted in underground mines in many countries, such as the United States (Katherine *et al.*, 2011), the United Kingdom (Brenkley *et al.*, 2013), Chile (Mejias *et al.*, 2014), Indonesia (Paul *et al.*, 2019), etc.. Some applications can be seen in Fig. 1.

(a) A 30-person MRC in UK (Brenkley *et al.*, 2013) (b) A 50-person MRC in USA (Trackemas *et al.*, 2015)

(c) A 80-person MRC in China (Li *et al.*, 2013) (d) A 300-person MRC in Indonesia (Paul *et al.*, 2019)

Fig. 1. Interior scenes of some MRCs in different countries.

Nomenclature

A	Body surface area, m^2	***Subscripts***	
c	Volume concentration	o	Oxygen
G	The O_2 supply rate, m^3/min	c	Carbon dioxide
h	Height of people, m	***Acronyms***	
M	Heat metabolic rate, W/m^2	AT	Ambient temperature
n	Number of people in a MRC	APD	air purification device
q	Per capita heat metabolic rate, W	ISRT	initial surrounding rock temperature
V	Volume of a MRC, m^3	MCA	Mine compressed air
v	Per capita metabolic rate	MRC	Mine refuge chamber
w	Weight of people, kg	PCM	Phase change materials
Greek symbols		RH	Relative humidity
τ	Unit time, min		

During the refuge process in a MRC, it is recognized that the physiological metabolism of personnel will consume O_2 accompanied by the production of heat, water vapor and harmful gases such as CO_2 and CO. This may expose the MRC to a dangerous environment of hypoxia, hot, humid and high concentration harmful gases (Bauer, *et al.*, 2009, Yantek *et al.*, 2019). Thus, in order to ensure environmental safety, some environmental control measures should be considered including oxygen supply, harmful gas scrubbing, dehumidification and cooling. However, the underground power is normally cut off due to disasters and mine electrical devices must be explosion-proof. As a consequence, it will become difficult to apply traditional air conditioning technology and equipment in MRCs.

Ambient temperature (AT) in a MRC is affected by the initial surrounding rock temperature (ISRT) as well as the heat transfer process between the surrounding rock and air (Yan *et al.*, 2020a). When the ISRT is over 20 °C, the cooling measure should be considered (Zhang *et al.*, 2018). Mechanical ventilation is a conventional method for controlling indoor relative humidity (RH) and AT, as well as air quality (Nitter *et al.*, 2020). For the environmental protection in a MRC, mine compressed air (MCA) generated from air compressors on surface and entering the MRC through a protected MCA pipeline or a borehole is the most effective and economical method. However, it is not practical to employ boreholes to deliver air to MRCs for some mines due to drilling costs, difficult terrain and surface rights issues (Trackemas *et al.*, 2015). In addition, the borehole is not suitable for MRCs with a buried depth of more than 400 m. This is due to the reason that the earth-air heat exchange in the long vertical borehole can significantly reduce the indoor AT while it only has a lag effect on the air humidity ratio, causing the indoor thermal discomfort with a high RH (Gao *et al.*, 2020). Several studies indicated that, when MCA is used in a MRC, the per capita air volume of 42 L/min can meet the oxygen-supply demand (Shao *et al.*, 2016), 100 L/min can meet the CO_2-scrubbing demand (Zhang *et al.*, 2019) and the cooling demand in a MRC with an ISRT of 24 °C, 300 L/min can meet the temperature control demand of a MRC with an ISRT of 27 °C within 96 h (Zhang *et al.*, 2020).

For most underground mines in China, MCA is mainly sent into MRCs via a protected MCA pipeline. Considering that the MCA pipeline may be damaged in the event of an accident, and it will take time to repair it. Therefore, in addition to the MCA, at least one backup measure is needed for O_2 supply and harmful gas scrubbing. In terms of O_2 supply, the high-pressure oxygen cylinder is a more convenient and safe alternative measure compared with chemical oxygen such as an oxygen candle. In terms of harmful gas scrubbing, methods of active chemisorption through air purification device (APD) and passive chemisorption through chemical adsorbent curtains have been proposed (Bauer *et al.*, 2009), but previous studies mainly focus on the development of chemical adsorbent materials and APDs. Some existing or newly synthesized chemical materials, including KO_2 oxygen plate (Gao *et al.*, 2015), g-C_3N_4 foam/Cu_2O QDs (Sun *et al.*, 2019), soda lime (Yantek *et al.*, 2019), modified soda lime (Du *et al.*, 2018, Gai *et al.*, 2019), $Ca(OH)_2$ (Moreno *et al.*, 2021) and amine-based modified porous material (Zhang *et al.*, 2021), etc., have been used as CO_2 adsorbents. Noble metal catalysts (e.g. PD-1, AU-1) and non-noble metal catalysts such as Hopcalite have been selected to scrub CO (Jia *et al.*, 2014). Taking into account the failure of underground power supply, some air-conditioning equipment with only harmful gases scrubbing function, driven by battery-operated fans (Bauer *et al.*, 2009; Du *et al.*, 2017), man-operated fans (Bo, 2014) or pneumatic fans (Zhang *et al.*, 2017), have been developed for low-temperature MRCs. Meanwhile, some air-conditioning equipment combined with cooling, dehumidification, and air purification has also been developed for high-temperature MRCs (Yang *et al.*, 2013). Zhang *et al.* (2017) conducted a simulation experiment in a 50-person MRC in which APDs filled with $Ca(OH)_2$ particles were used to scrub CO_2. Their experimental results showed that under the condition of a per capita CO_2 metabolic rate of 0.5 L/min, two selected APDs can make the indoor average CO_2 concentration below 0.8%.

As far as the AT control is concerned, it has been confirmed that for MRCs with an ISRT of above 27 °C, it is difficult to achieve the temperature control requirement within 96 h by MCA alone. In recent years, some cooling technologies, such as phase change material (PCM) cooling (Wu *et al.*, 2012), liquid CO_2 cooling (Yang *et al.*, 2013), ice storage cooling (Jia *et al.*, 2015, Du *et al.*, 2017, Shu *et al.*, 2017, Xu *et al.*, 2017), PCM combined with pre-cooling of the envelope (Yuan *et al.*, 2017, Gao *et al.*, 2017, Gao *et al.*, 2018) and liquid air cooling (Yan *et al.*, 2020b) have been developed and applied widely. These cooling technologies have a commonality, that is, store the cold sources at ordinary times and release the cold sources at a lower cost when people take refuge in order to achieve the indoor temperature control in a MRC. PCM cooling is suitable for MRCs with low ISRT (Wu *et al.*, 2012). Liquid CO_2 cooling technology has a poor cooling effect in an environment with the AT above 32 °C accompanied by a risk of leakage. Ice storage cooling technology has a wide range application prospect, but the supporting refrigeration compressor is easily broken in a place with high temperature and humidity. In addition, the supporting circulating fan needs to rely on other power, which reduces the reliability of the system. The cryogenic liquid air system is suitable for high-temperature MRCs, but with high technical requirement of maintaining liquid air at -195 °C and high costs from \$75 K to \$110 K (Yan *et al.*, 2020b).

It appears from the previous investigations that most of the work mainly focused on the environmental protection characteristics of MCA used in MRCs, the development of adsorption materials, APD, and cooling technology to cope with the failure of the MCA. However, there are few real human experiments carried out to investigate the human metabolic parameters and the application performance of the environmental control measures in MRCs with large capacity during the refuge process. In the current work, an 8-hour human experiment in a 50-person MRC will be carried out to better understand the metabolic parameters of personnel during the refuge process and the effectiveness of environmental protection measures in the MRC. Through monitoring the variation of gas concentration, AT and RH with time, the metabolic parameters of personnel and the operating characteristics of air conditioning devices in the MRC can be obtained. In addition, the possibility of passively scrubbing CO_2 through $Ca(OH)_2$ bags will be also investigated through simulation experiments in a MRC.

2 Materials and Methods

2.1 *Experimental environment*

The experiment was carried out in a 50-person MRC laboratory located in Beibei District, Chongqing City of China. Although the MRC laboratory is built on the ground, it can simulate the real interior scene of an underground MRC for 50 people in full scale. The space of the MRC laboratory is divided into three areas including two transition rooms and one living room. A two-door structure that opens outward is used, among them, the first door adopts a protective closed door that can resist shock waves and block toxic gases, while the second door uses a closed door which can only block toxic gases. The effective pass size of these doors is 0.8 m×1.6 m. The groove around the door wall has a depth of not less than 0.2 m, and the wall is poured by concrete with a strength not lower than C30 to ensure sufficient airtightness. The pouring thickness of the explosion-proof wall and the enclosed wall are 0.8 m and 0.3 m, respectively. The ground, arched roof and both-side walls of the MRC are poured with concrete, their thickness are 0.4 m, 0.5 m and 0.3 m, respectively. To facilitate the passage of personnel and equipment, the same entrance is set on both sides of the MRC. The living room occupies the arched space between the two enclosed walls with a cross-section of 4 m in width, 3.5 m in height, 14 m in circumference, 13.2 m^2 in area, 17 m in length and 224.4 m^3 in volume. There are 27 triple seats placed near one side wall of the room. A step is constructed with a steel plate on the wall near the seat above the ground 1.2 m, which is used to place 10 sets of MCA self-rescue devices for 50 people. Along the bottom of the step, 25 lamp bases are installed for heating lamps (200 W each lamp) to simulate the heat dissipation of human metabolism. The scene of the MRC laboratory is shown in Fig. 2.

(a) outside **(b) Interior**

Fig. 2. Scene of the MRC laboratory.

2.2 *Subjects*

The miners who benefit from a MRC are normally adult men, who are regarded as subjects in the current research. 50 subjects with age ranging from 28 to 45, and 80% of them are 30~40 years old. The height of most subjects ranges from 1.68 m to 1.76 m. The subjects are all healthy and they did not participate in alcohol activities before each experiment. Moreover, smoking and drinking are forbidden during the experiment. During the test period, adequate mineral water, compressed biscuits, and beef jerky, as well as two portable toilets are prepared to facilitate the diet and excretion of subjects.

2.3 *Instruments and equipment*

Before the experiment, 8 oxygen cylinders with 40 L and 20 MPa are prepared in the transition room to supply O_2 gas. The structure principle of the O_2 supply system is shown in Fig. 3. The O_2 gas flow rate is adjusted by a control cabinet and measured by a float flowmeter. There are three devices combined with functions of air purification, dehumidification and cooling to protect the environment in the living room. The working principle of these devices is to divert polluted air from the living room into the device through a circulating fan and sequentially pass through an air purification module using chemical adsorption and a cooling and dehumidifying module using evaporative cooling. Then the treated fresh air returns to the living room from the air outlet of the circulating fan, the structure principle of the APD is illustrated in Fig. 4. The air inlet is a rectangular surface with 0.4 m×0.6 m, and the air outlet is a circular surface with a radius of 0.05 m. It is worth mentioning here that the device is equipped with two circulating fans. One is powered by a CO_2 airflow, the liquid CO_2 from the compressed cylinders is decompressed twice to achieve phase change refrigeration for a MRC that requires cooling measure. And the decompressed CO_2 airflow enters the circulating fan to drive it works, then is discharged to the outdoors through the draft tube. The other fan powered by MCA or compressed air cylinders is mainly used in a MRC where the cooling measure is not required.

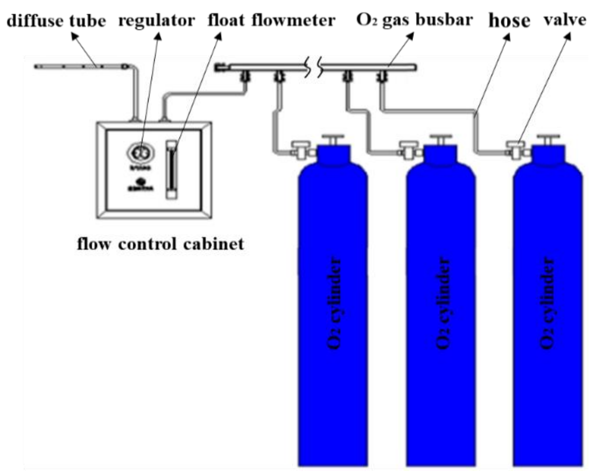

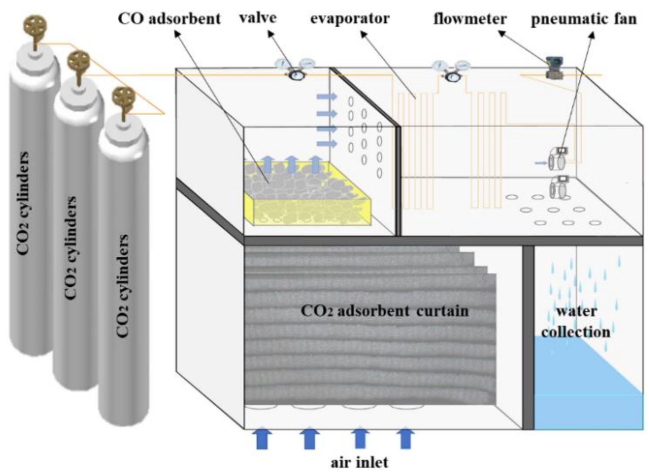

Fig. 3 Structure principle of the O_2 supply system **Fig. 4. Structure principle of the APD.**

The experiment was carried out on a certain day in January, from 9:30am to 6:30pm. During the experiment, the outdoor AT was 10 °C ~ 15 °C. It has been preliminarily evaluated that the AT in the living room will not exceed 30 °C without cooling requirement and the CO concentration will be below 24 ppm without scrubbing measure during the experiment. Therefore, compressed liquid CO_2 were not used for refrigeration and CO adsorbents were not used to scrub CO, only CO_2 adsorbents were added to the device to scrub CO_2. The circulating fan of the device was driven by a compressed airflow with 0.3 MPa from an air compressor. The air velocity at the outlet of the circulating fan was 10±0.5 m/s measured by an anemometer. Considering the chemical adsorbent used to scrub CO_2 in common for MRCs, the CO_2 adsorbent used in the experiment is $Ca(OH)_2$ particles, which are made into a curtain shape so that they can be quickly filled or replaced. Each curtain contains 3 kg $Ca(OH)_2$ particles, which must be stored in a vacuum seal before use. Each time the adsorbent needs to be added or replaced, each device consumes five curtains.

2.4 *Data collection*

In the living room, three measuring points for CO_2, O_2, CO and CH_4, as well as two measuring points for RH are arranged on both sides of the wall about 1.5 m above the ground, 5 measuring points for AT are arranged at 1 m to 2.5 m height above the ground, the distribution of subjects, devices, and measuring points is shown in Fig. 4, information of sensors used for different parameters can be seen in Table 1.

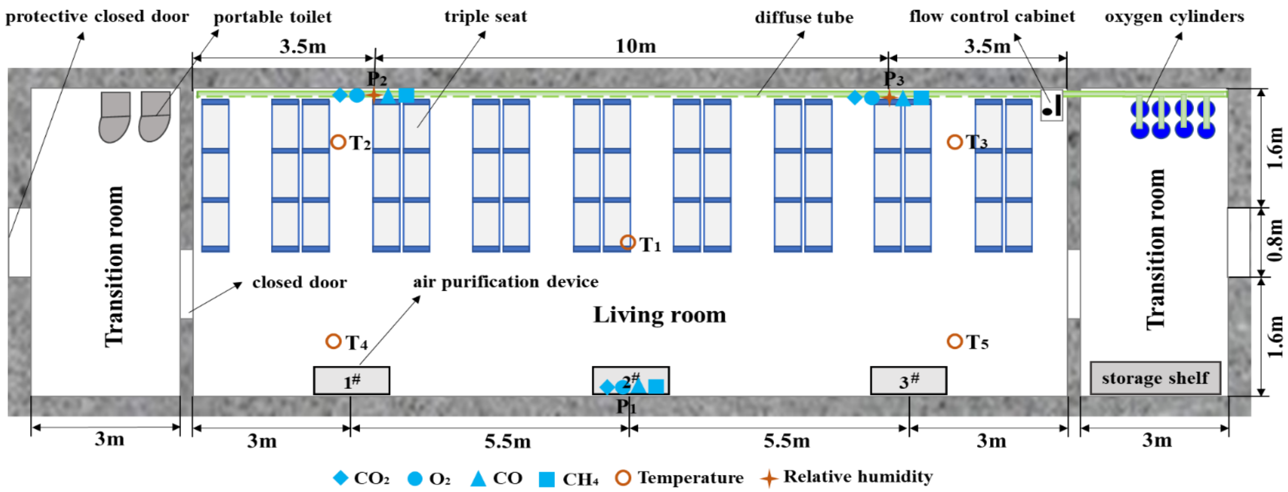

Fig. 4. The distribution of indoor subjects, devices and measuring points.

Table 1. Information of sensors used for different parameters

Parameters	Instrument/Model	Range	Accuracy	Manufacturer
CO_2 concentration	Mine infrared carbon dioxide sensor, GRG5H	0~5%	0.1%	
O_2 concentration	Mine oxygen sensor, GYH25	0~25%	0.1%	CCTEG Chongqing
CH_4 concentration	Mine methane sensor, KG9701B	0~4.00%	0.1%	Research Institute
CO concentration	Mine carbon monoxide sensor, GTH1000	0~1000 ppm	1 ppm	Co., Ltd.
RH	Mine temperature & humidity sensor, GWSD50/100	0 ~ 100%	0.1%	
AT	Platinum thermal resistance, PT100	-100 ~ 300 °C	0.1 °C	ELECALL Co., Ltd.

The data monitored by these sensors is uploaded to a data acquisition system platform through multi-channel recorders. The scene of the platform and the interface of the data acquisition system are shown in Fig. 5 (a) and (b), respectively.

(a) Parameter test platform **(b) Interface of the acquisition system**

Fig. 5. Scene of the platform and the interface of the data acquisition system.

2.5 ***Experimental procedure***

During the experiment, the subjects are in a sitting or light work state. To determine the per capita metabolic rate when people take refuge, the indoor CO_2 and CO concentrations are in a natural rising state at the early stage of the experiment. When the average CO_2 concentration is close to 1%, the CO_2 absorbent will be added to the APDs to scrub CO_2 gas. During the experiment, the APDs went through three different operating conditions to test their performance, and the O_2 supply rate was adjusted in time to adapt to changes in O_2 concentration. Fig. 6 shows the experimental scene at a certain moment after the heater lamps are switched on.

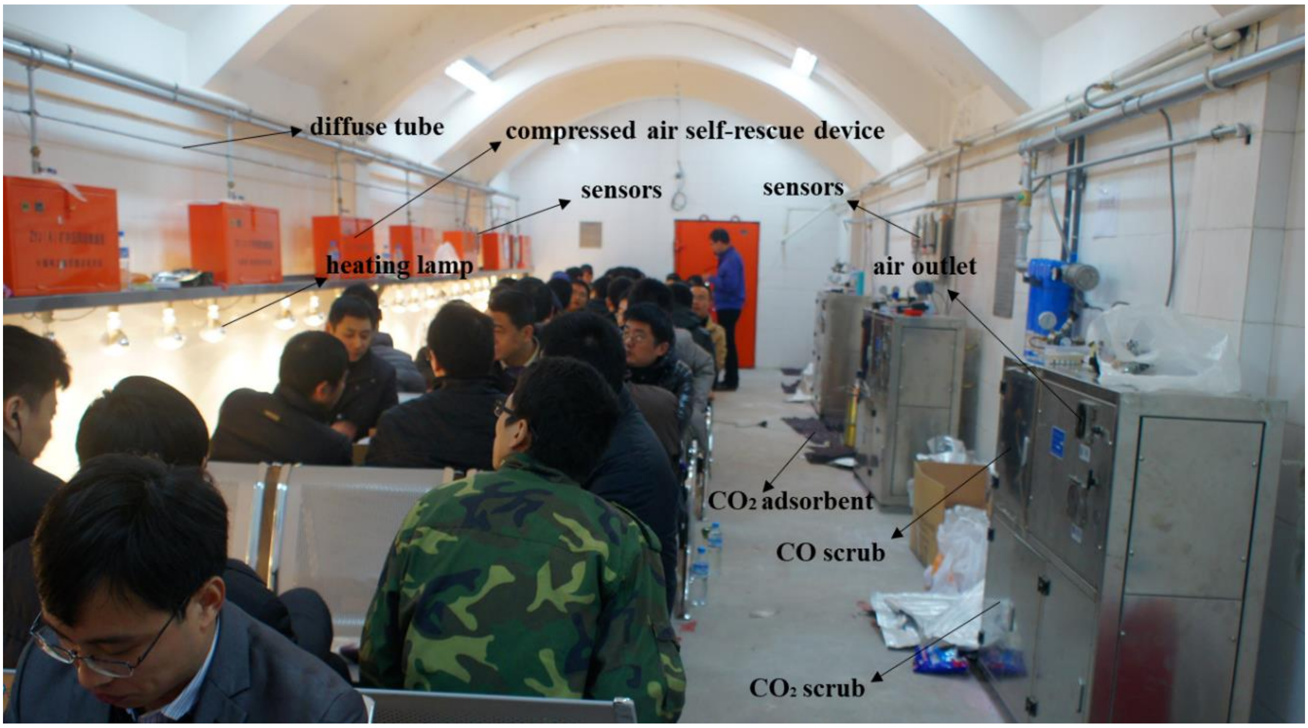

Fig. 6. Experimental scene of 50-person refuge test.

The main operating steps during the experiment are as follows:

(1) Before the experiment, open the data acquisition system for 0.5 h to obtain initial environmental parameters.

(2) All subjects quickly enter the living room, then close airtight doors on both sides.

(3) Open the O_2 supply system and adjust the flow to 40 L/min.

(4) Turn on the 3 sets of devices without filling the CO_2 adsorbent to stir to make the air distribution more even.

(5) At about 1.2 h, adjust the O_2 supply flow to 30 L/min, since the indoor O_2 concentration rises faster.

(6) At about 2 h, add CO_2 adsorbent to the $1^{\#}$ and $3^{\#}$ devices, since the CO_2 concentration is close to 1%.

(8) At about 4.8 h, replace CO_2 adsorbent in the $1^{\#}$ and $3^{\#}$ devices, and add CO_2 adsorbent to the $2^{\#}$ device.

(7) At about 5.3 h, adjust the O_2 supply flow to 20 L/min, because the O_2 concentration keeps rising.

(9) At about 6.6 h, adjust the O_2 supply flow to 10 L/min, and turn on the heating system.

(10) When the test lasts about 8.5 h, end the experiment and save the recorded data.

3 Results

3.1 ***Oxygen concentration***

Fig. 7 plots the variation of O_2 concentration in the MRC with time under four different operating conditions, i.e., O_2 supply rates of 40 L/min within 0~1.2 h, 30 L/min within 1.2~5.3 h, 20 L/min within 5.3~6.6 h, and 10 L/min within 6.6~8.5 h, respectively. The corresponding per capita O_2 supply rates are 0.8, 0.6, 0.4 and 0.2 L/min. From Fig. 7, it can be observed that, under the four different O_2 supply states, the O_2 concentration varies approximately linearly with time, which demonstrates that during the refuge process, the O_2 consumption rate of human metabolic is relatively stable. The values of O_2 concentration at points 2 and 3 are very close, while at point 1 is larger, the maximum difference at a certain moment is close to 0.7%. This phenomenon may be caused by the fact that point 1 is far away from the subjects while both points 2 and 3 are located above the crowded areas and closer to the oxygen-supply diffuse tube. When the per capita O_2 supply rate reaches 0.8 L/min, the O_2 concentration increases quickly with time, which means that the indoor O_2 supply rate greatly exceeds the O_2 consumption rate by personnel. When the per capita O_2 supply rate reduces to 0.5 L/min per person within 1.2~5.3 h, the O_2 concentration curve is still on the rise, but the growth gradient has decreased. This indicates that the per capita O_2 metabolic rate in the MRC is less than 0.5 L/min. It should be noted that during 2.5~3.5 h, the indoor O_2 concentration increase rate is relatively slow due to the subjects having lunch. When the per capita O_2 supply rate reaches 0.4 L/min per person within 5.3~6.6 h, the O_2 concentration curve changes smoothly. Whereas when the O_2 supply rate reduces to 0.2 L/min per person, the variation of O_2 concentration with time becomes a downward trend. It can be deduced that the per capita O_2 metabolic rate ranges from 0.2 L/min to 0.4 L/min.

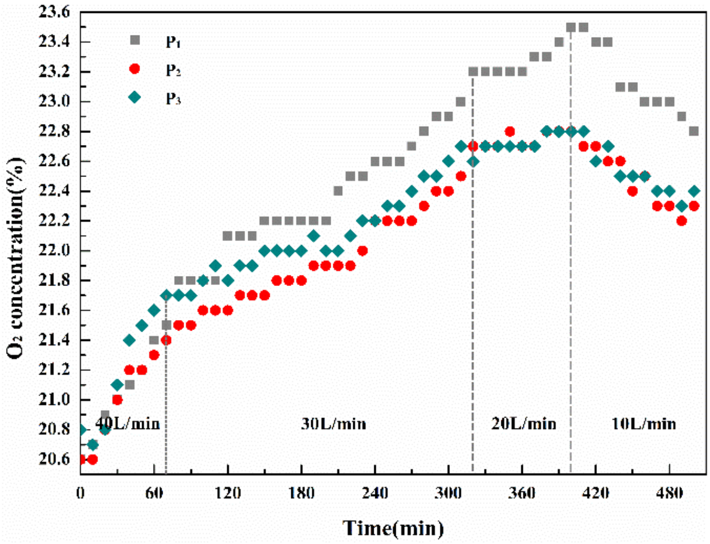

Fig. 7. O_2 concentration varies with time.

3.2 *Carbon dioxide concentration*

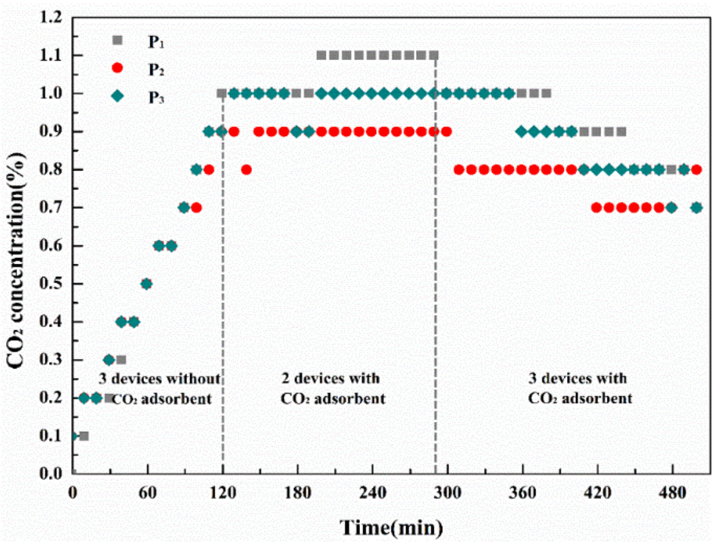

Fig. 8. CO_2 concentration varies with time.

Fig. 8 presents the variation of CO_2 concentration in the MRC with time under three different conditions, such as three APDs operate without CO_2 adsorbent within 0~2 h, two APDs with CO_2 adsorbent operate within 2~4.8 h and three APDs with CO_2 adsorbents operate within 4.8~8.5 h. It can be seen clearly that, for the cases of three APDs are operated without CO_2 adsorbent, the CO_2 concentration approximately linearly varies with time. The CO_2 concentration increased to about 1% after the 50 objects entered the living room for 2 h. When the CO_2 adsorbent is filled into two APDs, the CO_2 concentration is maintained at a relatively stable value ranging from 0.9% to 1.1%, which implies that two APDs used in this test can meet the control demand of CO_2 concentration for a 50-person MRC. When three APDs filled with CO_2 adsorbent are operating in the 50-person MRC, the indoor CO_2 concentration gradually decreases with time, the CO_2 concentration value stabilizes at about 0.7% after 2 h.

3.3 *Carbon monoxide concentration*

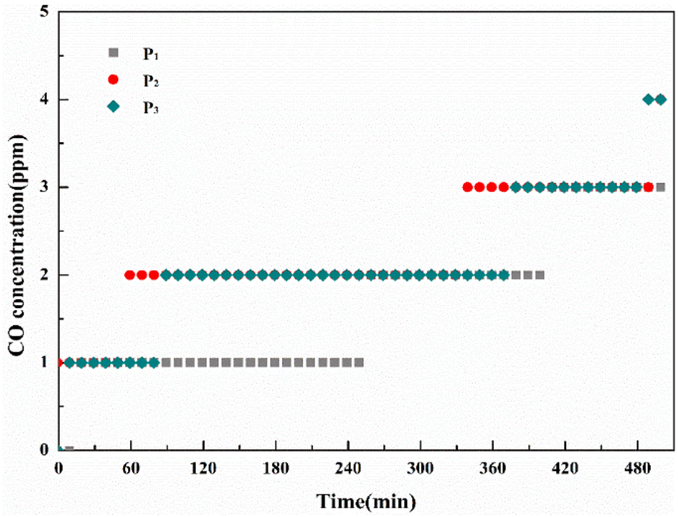

Fig. 9. CO concentration varies with time.

Fig. 9 demonstrates the variation of CO concentration with time in the MRC without CO scrubbing measure. It can be found that the CO concentration increases monotonically with time, but after 8.5 h, the CO concentration only increased by about 4 ppm. It can be inferred that the CO concentration in the MRC may increase to about 45 ppm at 96 h, the CO concentration will exceed the allowable value of 24 ppm by the current standard.

3.4 *Methane concentration*

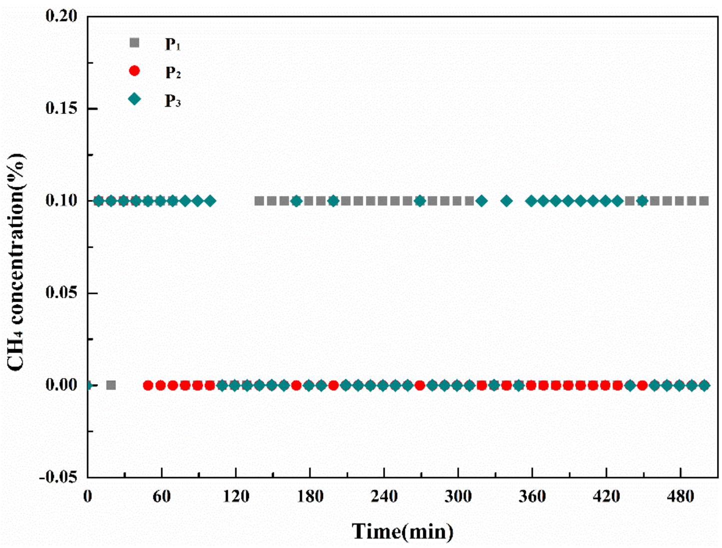

Fig. 10. CH4 concentration varies with time.

Fig. 10 plots the variation of CH_4 concentration with time in the MRC without CH_4 scrubbing measure. It can be found that the CH_4 concentration oscillates between 0 and 0.1%. This phenomenon occurs mainly because the accuracy of the methane sensor is 0.1%, and there is almost no CH_4 gas produced in the process of human metabolism. According to the result, the changes in air quality caused by the CH_4 gas generated from human metabolism could be ignored within 96 h for a MRC.

3.5 *Ambient temperature*

During the experiment, the MRC went through three periods with different thermal intensities. That is, there is only human metabolic heat within 0~2h, the chemical reaction heat between CO_2 and $Ca(OH)_2$ is increased within 2~6.3 h, and an additional heat of 5 KW is increased within 6.3~8.5 h by the 25 heating lamps.

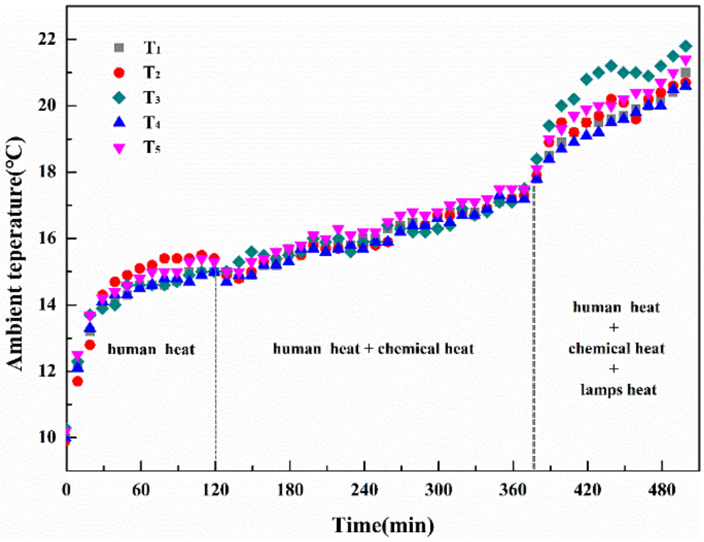

Fig. 11. AT varies with time.

Fig. 11 presents the variation of AT in the MRC with time. It should be noted that the AT quickly rises to 14 °C from 10 °C during 0.5 h followed by a slight increase of AT. From 1 h to 2 h, the average AT rises to 15.14 °C from 14.74 °C, the gradient of AT rise is about 0.40 °C/h. It can be found that the AT curve fluctuates slightly within 2~3 h. This could be the reason that when the CO_2 adsorbent is added to the devices and food is distributed to the subjects, the movement of some subjects indoors could lead to some interference to the measured value of these measuring points. From 2 h to 6.3 h, due to the increase in chemical reaction heat between water vapor, CO_2, and $Ca(OH)_2$, the gradient of AT shows a slight increases compared to that within 1~2 h. The average AT rises to 17.25 °C at 6 h from 15.6 °C at 3 h, the gradient of AT rise is about 0.55 °C/h. When the additional 5 KW heat intensity suddenly is increased by heating lamps at 6.5 h, the AT rises significantly in less than 0.5 h, then the gradient of AT rise drops again, the average AT rises from 19.74 °C at 7 h to 20.97 °C at 8.5 h, the gradient of AT rise is about 0.82 °C/h.

In the current experiment, there is no external ventilation, therefore, the heat generated by subjects and devices is mainly absorbed by the indoor air and walls. It can be deduced from Fig.11 that when the heat intensity suddenly increases, the AT will rise rapidly in a short period that is less than 0.5 h, then the AT increase rate will gradually decrease until it tends to be a relatively balanced state. The reason for this phenomenon is that when the indoor heat intensity increases suddenly, the heat exchange rate between the air and the wall is relatively small due to the small temperature difference, except the heat absorbed by the wall, the excess heat is absorbed by the air with a relatively small specific heat capacity so that the AT rises rapidly. As the AT increases, the temperature difference between the air and the wall increases, and the heat absorbed by the wall increases until it is almost equal to the indoor heat generation. It can be inferred from this that, in a MRC, the heat exchange between the surrounding rock and the air has an important influence on the control effect of the AT, the gradient of AT rise is positively correlated with the indoor heat intensity.

3.6 *Relative humidity*

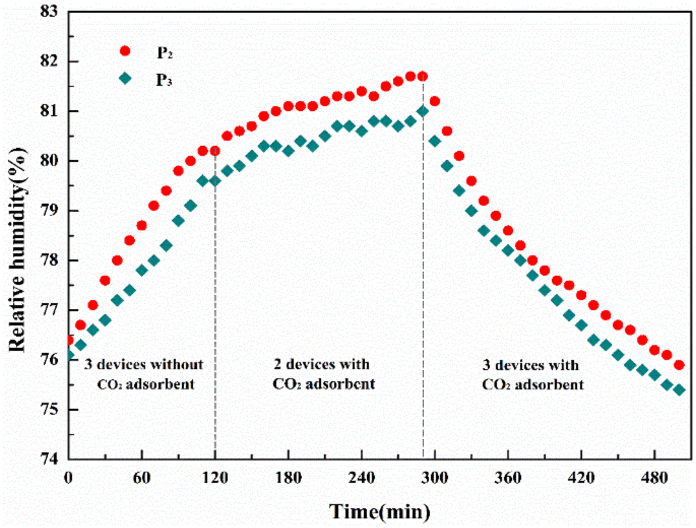

Fig. 12. RH in the MRC varies with time.

Fig. 12 plots the variation of RH in the MRC with time. It can be found that in the first two hours, the RH increased relatively quickly, from 76.2% to 79.5%. When two APDs filled with CO_2 adsorbents operate from 2 h to 4.8 h, the gradient of RH decreased slightly since the water vapor reacted with $Ca(OH)_2$ particles and are absorbed. The RH slowly increases to approximately 81% in nearly 3 h. When the three devices are used from 4.8 h, the RH in the MRC starts to drop, and the RH reaches approximately 76% within 3 h, meeting the requirement of RH control in the MRC. This means that APDs can control RH and CO_2 concentration at the same time for MRCs.

4 Discussion

4.1 *Metabolic parameter of refugees*

The main control parameters of human metabolism such as the metabolic rates of O_2, CO_2 and heat can be calculated from the experimental data.

When the O_2 gas is supplied only through compressed oxygen cylinders in the MRC, and the APDs are running without chemical adsorbents. According to the law of conservation of matter, there is

$$V\frac{\partial c_o(\tau)}{\partial \tau} = G(\tau)\text{-}nv_o(\tau)\times 10^{-3} \tag{1}$$

where V is the volume of the MRC, m^3; τ is the unit time, min; c_o is the O_2 concentration; G is the O_2 supply rate, m^3/min; n is the number of people in the MRC; v_o is the per capita O_2 metabolic rate, L/min.

Thus, the per capita O_2 metabolic rate can be calculated as

$$v_o(\tau) = \left[G(\tau)\text{-}V\frac{\partial c_o(\tau)}{\partial \tau}\right]\times 10^3 \Big/ n \tag{2}$$

When there are no CO_2 scrubbing measures in the MRC, the indoor CO_2 concentration is only affected by the CO_2 metabolism of personnel. According to the law of conservation of matter, there is

$$V\frac{\partial c_c(\tau)}{\partial \tau} = nv_c(\tau)\times 10^{-3} \tag{3}$$

where c_c is the CO_2 concentration; v_c is the per capita CO_2 metabolic rate, L/min.

Thus, the per capita CO_2 metabolic rate can be calculated as

$$v_c(\tau) = V\frac{\partial c_c(\tau)}{n\partial \tau}\times 10^3 \tag{4}$$

The heat metabolic rate is determined by the measured per capita O_2 metabolic rate, the per capita CO_2 metabolic rate, and the body surface area, it can be indirectly calculated as follows (Zhai *et al.*, 2018)

$$M = \left(0.23v_c + 0.77v_o\right) \times 5.88 \times 60 / A \tag{5}$$

where M is the heat metabolic rate, W/m^2; A is the body surface area, m^2.

The body surface area can be determined using the following formula (Shimazaki and Katsuta, 2019)

$$A = 0.2w^{0.425} \times h^{0.725} \tag{6}$$

where w is the weight of people, kg; h is the height of people, m. For Chinese adult men, the average value is 1.80~1.83 m^2;

(1) O_2 metabolic rate

As far as the O_2 metabolic rate is concerned, in the current experiment, the use of compressed oxygen bottles to supply oxygen is the only measure. Once the value of O_2 supply at each stage is determined, then the average oxygen metabolic rate of each stage can be theoretically calculated. However, from the experimental results, the relative deviation of the three measurement points after 5.3 h is relatively large. Therefore, according to Eq. (2), it is more appropriate to use the experimental data of the first two stages before 5.3 h as the calculation basis. The oxygen supply flow rate is 40 L/min from 0 to 1.2 h and 30 L/min from 1.2 to 5.3 h, respectively. The indoor average O_2 concentration of the three measuring points is 20.77% at 0 h, 21.53% at 1.2 h and 22.77% at 5.3 h, respectively.

From 0 to 1.2 h, the per capita O_2 metabolic rate in the MRC can be calculated as

$$v_o(\tau) = \left[G(\tau) \text{-} V\partial\frac{c_o(\tau)}{\partial\tau}\right] \Big/ \mathrm{n} = \frac{40\times1.2\times60 - 224.4\times10^3\times(21.53\% - 20.77\%)}{50\times1.2\times60} \approx 0.33 \ \text{ L/min}$$

From 1.2 to 5.3 h, the per capita O_2 metabolic rate in the MRC can be calculated as

$$v_o(\tau) = \left[G(\tau) \text{-} V\partial\frac{c_o(\tau)}{\partial\tau}\right] \Big/ \mathrm{n} = \frac{30\times(5.3\text{-}1.2)\times60 - 224.4\times10^3\times(22.77\% - 21.53\%)}{50\times(5.3\text{-}1.2)\times60} \approx 0.37 \ \text{ L/min}$$

It can be found that the O_2 metabolic rate increased slightly within 1.2~5.3 h compared with that within 0~1.2 h, this could be due to the diet of the subjects during this period.

(2) CO_2 metabolic rate

As far as the CO_2 metabolism rate is concerned, since the MRC has adopted air purification measures after 2 h, and several parameters of the air purification device such as purification efficiency are still unclear, the experimental results cannot be used as a valid reference value, according to Eq. (4). Therefore, values of CO_2 concentration without purification measures within 0~2 h are selected for per capita CO_2 metabolism. It can be found that the CO_2 concentration grows approximately linearly with time from 0 to 2 h, and the linear fitting formula is y= 0.09 +0.43x, with R^2=0.99. The indoor average CO_2 concentration of the three measuring points is 0.07% at 0h and 0.97% at 2 h. Thus, the per capita CO_2 metabolic rate in the MRC can be calculated as

$$v_c(\tau) = V\partial\frac{c_c(\tau)}{n\partial\tau} = \frac{224.4\times10^3\times(0.97\% - 0.07\%)}{50\times2\times60} \approx 0.34 \ \text{ L/min}$$

Thus, the per capita CO_2 metabolic rate is 0.34 L/min for Chinese people who are taking refuge in a MRC. Yang *et al.* (2020) observed that for adult men at lying and office activity levels, the CO_2 metabolic rates range from 0.23 to 0.34 L/min, which is more consistent with our experimental results.

(3) Heat metabolic rate

The calculation method of the human metabolic heat in Eq. (5) takes into account the surface area of the human body. But the surface area of each subject is different, so there is a slight gap in the amount of heat dissipation. Therefore, when we calculate the average heat dissipation rate of subjects, we consider that all subjects have the same metabolic parameter values and body surface area. Thus, when calculating the per capita heat metabolic rate in the MRC, according to Eq. (7), there is

$$q = M \cdot A = \left(0.23v_c + 0.77v_o\right) \times 5.88 \times 60 \tag{7}$$

Where q is the per capita heat metabolic rate, W.

Thus, from 0 to 1.2 h, the per capita heat metabolic rate in the MRC can be calculated as

$$q=(0.23\times0.34+0.77\times0.33)\times5.88\times60\approx117 \text{ W}$$

From 1.2 to 5.3 h, the per capita heat metabolic rate in the MRC can be calculated as

$$q=(0.23\times0.34+0.77\times0.38)\times5.88\times60\approx128 \text{ W}$$

Thus, for Chinese adult men, when they are taking in a MRC, the per capita heat metabolic rate ranges from 117 W to 123 W, which is consistent with the recommendation value of 113~134 W when people are resting in a refuge alternative (Bernard *et al.*, 2018).

(4) Sweat metabolic rate

Hirata *et al.* (2015) found that young men with an age of 20~30 exposed to the thermal environment with RH of 60% and temperature of 32.5 °C while standing for 3 h, the sweat metabolic rate is about 4.5 g/min. According to the result of Klein *et al.*, (2017), at an apparent temperature of 96.5 °F (35.83 °C), the moisture loss, from sweat and respiration, of 1.0 L/day for both the 78.5 kg and 111 kg humans with high body fat at an activity level of 1.0 met. During the refuge process, the activity levels of occupants in the MRC range from 0.8 to 1.0 met, the total moisture loss is less than 1 L/day per capita.

4.2 *Air quality control in MRC*

In terms of harmful gas scrubbing, the use of APDs must rely on external power, which will affect the reliability of the system to a certain extent. Although a method for passively scrubbing CO_2 through lithium curtains has been proposed (Bauer *et al.*, 2009), it has not been verified. Therefore, it is worth discussing whether the direct placement of chemical adsorbents in the MRC to passive scrub CO_2 meets the control requirement. A test was carried out in another MRC laboratory with a length of 20 m, a width of 4 m and a height of 3 m, as shown in Fig.13.

Fig. 13. remove CO_2 by adsorbent bags.

For more laboratory information, please refer to Zhang *et al.* (2020). During the test, the compressed CO_2 gas cylinders and diffuse pipes located on both sides of the room were used to simulate the CO_2 metabolism of 50 people, and the per capita CO_2 metabolic rate is 0.5 L/min. Before the test, the initial CO_2 concentration of the MRC laboratory is closed to 1.1%. $Ca(OH)_2$ particles used to scrub CO_2 are packed into a small sand cloth bag every 2 kg. Respectively, 40, 80, and 130 bags are hung on four shelves, at times of 0 h, 0.2 h, and 0.6 h, to passively control CO_2 concentration. There are five measuring points distributed in the room to monitor CO_2 concentration in real-time.

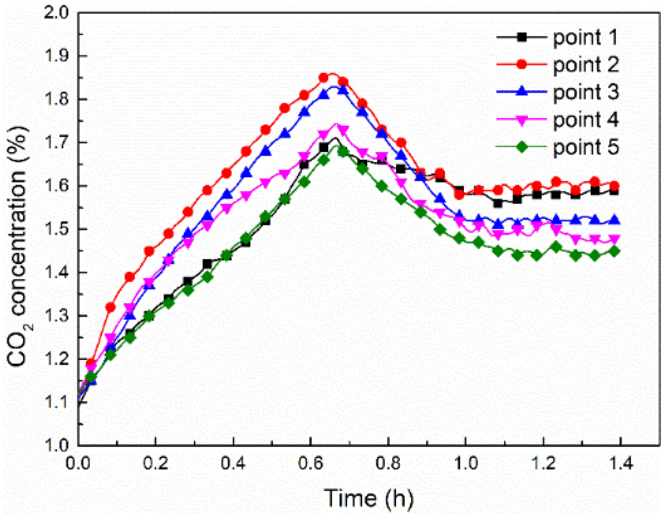

Fig. 14. CO_2 concentration varies with time.

Fig. 14 plots the variation of CO_2 concentration with time. It can be observed that when 40 bags of CO_2 adsorbent bags were used to scrub CO_2 gas in a 50-person MRC, the CO_2 concentration trends upward over time and the average value rises to 1.65% from 1.1% within 0.3 h. When the CO_2 adsorbent bags increase to 80 bags at 0.3 h, the rising trend of the CO_2 concentration slows down, and the average CO_2 concentration rises to 1.82% from 1.65% within 0.35 h. When the CO_2 adsorbent bags increase to 130 bags at 0.65 h, the CO_2 concentration shows a downward trend with time, and the average CO_2 concentration stabilizes at 1.52% after 0.4 h. According to the experimental result, it can be imagined that if the CO_2 adsorbent bags continue to increase, the CO_2 concentration can be controlled below 1%. However, directly hanging the CO_2 adsorbent bags will greatly increase the amount of the CO_2 adsorbent, compared to the use of APDs.

4.3 *Thermal environment control in MRC*

(1) RH control

From the experimental results, it can be seen that the RH control in a MRC can be achieved simultaneously with CO_2 concentration when chemisorption is used to scrub CO_2. In contrast, for lower storage RH (≤75%), carbonation contributes only by a small fraction to CO_2 capture, most of the CO_2 captured is probably dissolved or in the form of bicarbonate ions in the physisorbed water present in $Ca(OH)_2$ (Moreno *et al.*, 2021). In addition, in an initial high-temperature MRC where a cooling measure is required, dehumidification can also be achieved simultaneously with air cooling when refrigeration devices cool the circulating air through condensers (Yang et al., 2013). However, compared with these dehumidification methods, MCA is also the simplest measure for dehumidification in a MRC. Its principle is that the air from the external environment enters a high-pressure storage tank after being compressed by a compressor, and exchanges heat with the outside through the surfaces of the storage tank and conveying pipeline, to realize the compression, cooling and dehumidification of the high-humidity air, then the fresh air with low RH enters the MRC to dilute the high-humidity air to achieve the purpose of humidity control. The parameters of MCA that meet the requirement of RH control in a MRC is worth studying.

A dehumidification test through MCA was carried out in the laboratory, as shown in Fig. 15. According to the result of Klein *et al.*, (2017), the moisture loss of occupants in MRC is 0.86 L/day per capita for this test. An ultrasonic humidifier with a water vapor dissipation capacity of 1.8 kg/h was used to simulate the moisture dissipation of 50 people, and a high-power fan was used to stir the indoor air to promote better dispersion. Compressed air provided by an air compressor with a rated air volume of 10 m^3/min was sent to the MRC laboratory from air outlets located on both side walls. The volume rate of air supply is controlled by a pressure-reducing valve and measured by a vortex flowmeter. A humidity sensor is placed in the center of the room above the ground 1m to obtain the real-time value of RH. The AT and RH outside the MRC were 27°C-29°C and 74%-80%, respectively, during the period of this test. The initial RH in the MRC ranges from 85% to 90%, the compressed air supply rates for the MRC were 250 m^3/h, 300 m^3/h, and 400 m^3/h, respectively. The scene of the test is shown in Fig. 15.

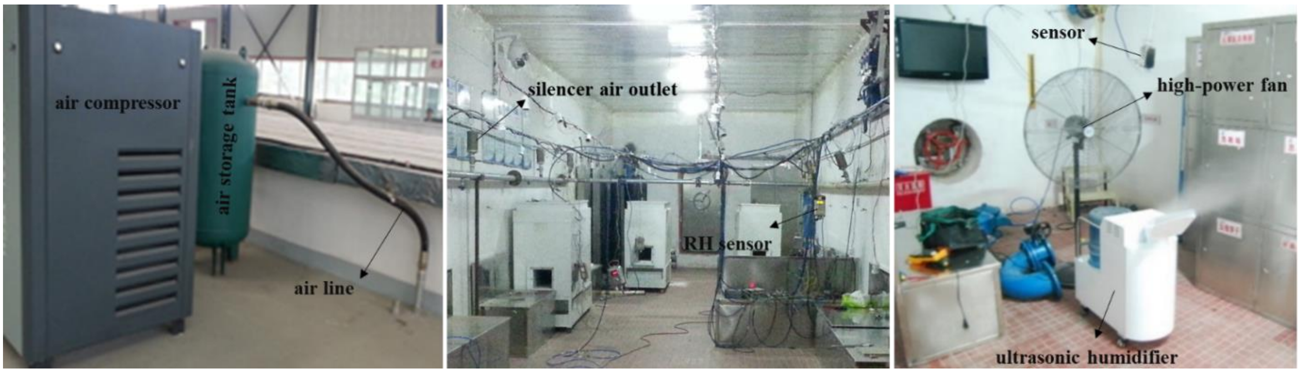

Fig. 15. RH in MRC varies with time under different ventilation rates.

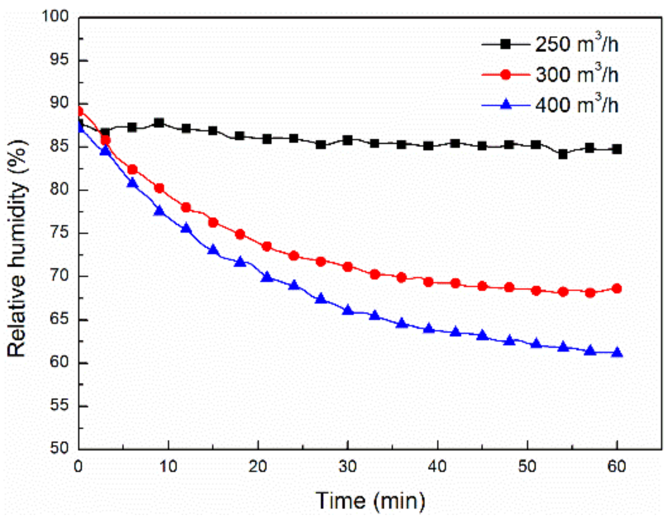

Fig. 16. RH in MRC varies with time under different ventilation rates.

Fig. 16 plots the variation of RH in the MRC with time under different ventilation rates. It can be found that when the air supply rate is 250 m^3/h, the RH drops from 88% to 85% within 1 h, and a relatively stable value is maintained. This basically satisfies the requirement of humidity control in the MRC, but the humidity should be improved in terms of comfort. When the air ventilation rate is increased to 300 m^3/h (0.1 m^3/min per capita), the RH in the MRC further drops and remains at about 68% from 89% in 1 h, the wet environment has been significantly improved. When the air supply rate increases to 400 m^2/h, the RH dropped from 88% to 61% in 1 h, which is close to the relatively comfortable range. It should be noted that the RH does not decrease linearly with the air supply rate. From the result of this test, it can be seen that in a MRC with compressors on the ground to provide MCA, when the per capita air volume is above 0.15 m^3/min, it is easy to control the RH below 60%.

(2) AT control

When calculating the heat load in a MRC, although the heat metabolic rate of each individual is slightly different under the same activity intensity, in terms of the heat metabolic rate during the refuge period, it is relatively reasonable to take the value of 120~130 W per capita. In addition, when chemical absorbents are used to scrub CO_2, an exothermal chemical reaction heat of 40~50 W cannot be ignored (Halim *et al.*, 2019). It is worth noting that the dynamic heat transfer between the surrounding rock and the air in MRC has an important influence on temperature control. Our previous studies showed that, for a MRC located in sandstone with ISRT less than 20 ℃, the AT can be passively controlled to not exceed 32 ℃ within 96 h due to the low-temperature surrounding rock (Zhang *et al.*, 2018). For a MRC located in sandstone with an ISRT of 24 ℃, the AT can be controlled below 32 ℃ within 96 h by relying on the MCA of 0.3 m^3/min per capita (Zhang *et al.*, 2019). For a MRC with a slightly higher ISRT, MCA and PCM cooling can be combined to achieve the temperature control goal. For a MRC with higher ISRT, technologies such as ice storage cooling, MCA composited ice storage cooling, or surrounding rock pre-cooling composited MCA, PCM cooling or ice storage cooling can be used to achieve the temperature control goal. However, the applicable scope and economy of these methods need to be investigated.

4.4 ***Acceptable range of environmental parameters***

As far as the safety is concerned, it is permissible for personnel to be exposed to a CO concentration of 50 ppm for 8 h according to the *Occupational Safety and Health Guideline for Carbon Monoxide*. Although humans exposure to a CO concentration of 400 ppm within 1 h may cause headaches, they dose not face the risk of death (Downs, 2016, Lee *et al.*, 2020). It has been inferred that the CO concentration in a MRC caused by human metabolism is below 50 ppm within 96 h, as a result, the environmental hazards caused by human metabolism of CO can be ignored. Considering that harmful gases with high CO concentrations in the roadway may influx into the MRC with the entry of people, in China, scrubbing measures must be equipped in the MRC to reduce the CO concentration from 400 ppm to 24 ppm within 20 minutes. Fresh air ventilation is the most direct and effective measure to dilute harmful gases. However, according to the calculation method (Zhang *et al.*2020), when the per capita ventilation rate is 0.3 m^3/min, it will take 30 minutes for MRC to reduce the CO concentration from 400 ppm to 24 ppm. If the requirement for rapid CO dilution within 20 minutes is met, the per capita ventilation rate should reach 0.45 m^3/min. Therefore, considering personnel safety and environmental control costs, it is recommended to increase the CO rapid dilution time to 30 minutes, or increase the allowable value of CO concentration to 50 ppm within 20 minutes.

In personnel exposure environments, CO_2 gas is usually used as a symbolic gas for evaluating indoor air quality (Zhu *et al.*, 2020), which affects human cognition and physiological safety. Although human is exposed to CO_2 at 0.3% or 0.4% for several hours results in decreased cognitive performance (Kajtár *et al.*, 2012), exposed to CO_2 at 0.5% within 2.5 h does not effect on acute health symptoms of respiratory, visual and skin-related, headache, and sensory (Zhang *et al.*, 2016). However, exposure to CO_2 at above 1% may lead to health symptoms of increased respiratory rate, respiratory acidosis, metabolic stress, increased brain blood flow, increased minute ventilation (Azuma *et al.*, 2018), and exposure to CO_2 at 1.2% with 32 °C WB and 85% RH led to significant headaches (Li *et al.*, 2018). For CO_2 concentration in MRC, the allowable value in the current documents is 1%. Whereas under the condition of a per capita ventilation rate of 0.3 m^3/min, the CO_2 concentration in a MRC can be maintained to a low level of 0.3% (Zhang *et al.*, 2020). Meanwhile, it is easy to reduce CO_2 concentration to below 0.5% through air APDs, according to our experimental results. From the perspective of rescue, keeping conscious during the evacuation period is more conducive to miners' judgment and escape. Therefore, it is recommended that the allowable value of CO_2 concentration can be limited to 0.5%, which will be acceptable in terms of economic costs.

The environment with AT above 32 °C and RH above 60% can be considered as a hot-humid environment (Shi *et al.*, 2013). The hot-humid environment has an important impact on human physiological health, in which the human body's heat dissipation is disrupted, leading to an increase in body temperature with a series of thermal symptoms and even death. Previous studies showed that exposure to RH at above 40% could be better for the eyes and upper airways than levels below 30% (Wolkoff *et al.*, 2007), and exposure to AT at 29 °C or below the heat sensation is not obvious. However, when the AT is above 30 °C with RH 70%, some subjects felt uncomfortable during 3 h exposure. When the AT reaches 32 °C, the human body feels warm, as the RH increases from 70% to 90%, the heat sensation becomes more and more obvious (Jin *et al.,* 2017). Hirata *et al.* (2015) found that young people with an age of 20~30 exposed to the thermal environment with RH of 60% and temperature of 32.5 °C while standing for 3 hours, the core temperature elevation in humans is 0.18 °C. In terms of the MRC where refugees will be continuously exposed for above 96 h, to maintain allowable values of AT and RH are very important. However, according to relevant documents of different countries, the allowable values in the MRC are different. In China, the allowable values of AT and RH are 35 °C in dry bulb and 85%, respectively (Yuan *et al.*, 2017). In the United States, the allowable value is apparent temperature 35 °C, namely, the AT is 28.5 °C when the RH is 85% (Halim *et al.*, 2019). In Indonesia, the allowable values are 32 °C WB and 65% RH, respectively (Paul *et al.*, 2019). Bernard *et al.* (2018) observed that an apparent temperature of 49 °C could be sustained for 24 h based on the predicted heat strain model. Ashley *et al.* (2019) found that sustainable exposures resulting in no significant increases in the physiological strain at an apparent temperature greater than 35 °C, with a likely ceiling below 46 °C AT. Hao *et al.* (2016) recommended a safe upper limit of 35 °C apparent temperature for 96 h with an upper limit AT of 29.6 °C at 90% RH. Thus, it can be seen that in terms of thermal environment parameters in a MRC, the allowable value is relatively moderate in Indonesia, but lower than that in the United States and higher than that in China. From the current results and previous research, it is easy to control the RH in a MRC below 60%, but for MRCs with higher ISRT, maintaining AT at a lower level means more cost. Considering personnel safety and cost, it is recommended that the RH and AT of MRC be limited to 60% and 32 ℃, respectively.

4.5 Recommended parameters for MRCs

Table 2 lists the recommended metabolic parameters and the environmental parameters for MRCs.

Table 2. Metabolic parameters and environmental parameters for MRCs

Terms	Specific parameter	Recommend from others	Our recommend
Values of main metabolic parameter during refuge	O_2 metabolic rate	0.29~0.37L/min for sitting men in Zhai *et al.*(2018)	0.33~0.37 L/min
	CO_2 metabolic rate	0.23 to 0.34L/min in Yang *et al.* (2020)	0.34 L/min
	Heat metabolic rate	113~134W in Bernard *et al.* (2018)	117~128 W
	Sweat metabolic rate	4.5g/min in Klein *et al.*, (2017)	1 L/day
Acceptable values of environmental parameters	O_2 concentration	18.5%~23% in Halim *et al.*, (2019)	18.5%~23%
	CO_2 concentration	1% in Halim *et al.*, (2019)	0.5%
	CO concentration	25ppm, from 400ppm to 25ppm within 20min in Halim *et al.*, (2019)	25 ppm, from 400 ppm to 25 ppm within 30 min
	Ambient temperature and relative humidity	35°C apparent temperature in Halim *et al.*, (2019), 32 °C WB and 65% RH in Paul *et al.*, (2019), 35°C WB and 85% RH in Yuan *et al.*, (2017)	32°C WB and 65% RH

5 Conclusions

In this research, an experiment of 50 subjects exposed in a MRC laboratory was carried out for 8.5 h to grasp the human metabolism during the refuge process and the characteristics of environmental control measures used in MRC. In addition, the possibility of passively scrubbing CO_2 through $Ca(OH)_2$ particle bags and the performance of dehumidification by MCA in the MRC were discussed by simulation experiments. Based on the results of these experimental studies, the following specific conclusions may be made.

(1) During the refuge period, the per capita metabolic rates of O_2, CO_2 and heat, are 0.38 L/min, 0.34 L/min and 130 W, respectively. The influence of trace gases such as CO and CH_4 produced by human metabolism on the indoor

MRC environment can be ignored.

(2) When $Ca(OH)_2$ particles are used as CO_2 adsorbents, the APD has the function of scrubbing CO_2 and dehumidification at the same time. Two devices can make the CO_2 concentration below 1% and the RH below 85%, and three devices can make the indoor CO_2 concentration below 0.8% and RH below 76%. The influence of the chemical heat caused by scrubbing CO_2 and dehumidification on indoor AT should not be ignored. Although the possibility of passively scrubbing CO_2 exists, when the $Ca(OH)_2$ particles are packaged to passively scrub CO_2, the amount of the adsorbent will increase significantly for MRC.

(3) When MCA is used to dehumidification in a MRC, the capita air volume of 0.1 m^3/min can control the RH below 80%, and 0.15 m^3/min per capita can maintain the indoor RH close to 60%.

(4) In the early stage of disaster avoidance, the indoor AT will rise rapidly within 1 h, and then slowly rise, the surrounding rock parameters have a significant impact on the rise of AT. Some composite temperature control schemes have been proposed for MRC with different initial surrounding rock temperatures.

(5) Considering the safety of human exposure for 96 h and the economy of environmental control, it is recommended that, for MRC, the allowable values of the indoor environmental parameters of CO concentration, CO_2 concentration, AT and RH are 50 ppm, 0.5%, 32 °C, and 60%, respectively.

Due to the limitation of the experimental environment, although the test carried out in this article is similar to the real situation of a MRC in terms of indoor air quality and humidity control. But for temperature control, there are certain differences in thermal properties between the concrete wall of the MRC laboratory and the surrounding rock of underground MRCs, also the variation of AT in the MRC laboratory may be affected by the external environment in the later stage. Therefore, regarding to the study of MRC temperature control, the thermal response tests will be conducted in an underground MRC in the future work. Apart from this, in terms of environmental protection in a MRC, there are still many issues worthy of in-depth study, e.g., how to achieve a better passive control of CO_2 concentration through chemical adsorbents, how to improve the reliability and economy of cooling methods, how to use the mine compressed air entering the MRC to rapidly control the indoor CO concentration. In the future work, investigations on the above aspects will be performed to realize reliable and inexpensive environmental protection technology for MRCs.

Acknowledgments

The authors would like to thank the financial support from the National Natural Science Foundation of China (NO. 52168013 and NO. 51908080). In addition, we would also like to thank the State Key Laboratory of the Gas Disaster Detecting, Preventing and Emergency Controlling, affiliated to Chongqing Research Institute of China, Coal Technology & Engineering Group, for providing support of experiment site and personnel.

Reference

Ashley, C., Lopez, R., Garzon, X., Bernard, T., 2019. Thermal exposure limit in a simulated refuge alternative. Mining Metall Explor. 37, 179-186. https://doi.org/10.1007/s42461-019-00134-3.

Azuma, K., Kagi, N., Yanagi, U., Osawa, H., 2018. Effects of low-level inhalation exposure to carbon dioxide in indoor environments: A short review on human health and psychomotor performance. Environ Int. 121, 51-56. https://doi.org/10.1016/j.envint.2018.08.059.

Bauer, E., Kohler, J., 2009. Update on refuge alternatives: research, recommendations, and underground deployment. Min Eng. 61, 51-57. https://www.cdc.gov/niosh/mining/UserFiles/works/pdfs/uorarr.pdf.

Bernard, T., 2012. Report on physiological analysis of human generated heat in a refuge alternative. Contract number: 254-2011-M-40932. The National Institute for Occupational Safety and Health, Office of Mine Safety and Health Research, 12 pp.

Bernard, T., Yantek, D., Thimons, E., 2018. Estimation of metabolic heat input for refuge alternative thermal testing and simulation. Min Eng. 70, 50-54. https://doi.org/10.19150/me.8429.

Bo, Z., 2014. Performance analysis and development of gas purifying device used in emergency refuge system. Coal Science and Technology. 42, 69-72. (In Chinese) https://doi.org/10.13199/j.cnki.cst.2014.07.018.

Brenkley, D., Gibson, D. , Espada, F. , Morillo, P., Fernández, M., Rodríguez, A., et al., 2013. Mine emergency support technologies. Technical Report. https://www.researchgate.net/publication/325466698.

Dou, S., Liu, J., Xiao, J., Pan, W., 2020. Economic feasibility valuing of deep mineral resources based on risk analysis: Songtao manganese ore-China case study. Resour Policy. 66, https://doi.org/10.1016/j.resourpol.2020.101612.

Downs, J., 2016. Carbon monoxide exposure: Autopsy findings. Encyclopedia of Forensic and Legal Medicine (Second Edition). 444-460. https://doi.org/10.1016/B978-0-12-800034-2.00058-6.

Du, Y., Gai, W., Jin, L., 2018. A novel and green CO_2 adsorbent developed with high adsorption properties in a coal mine refuge chamber. J Clean Prod. 176, 216-229. https://doi.org/10.1016/j.jclepro.2017.12.019.

Du, Y., Gai, W., Jin, L., Sheng, W., 2017. Thermal comfort model analysis and optimization performance evaluation of a multifunctional ice storage air conditioning system in a confined mine refuge chamber. Energy. 141, 964-974. https://doi.org/10.1016/j.energy.2017.09.123.

Gai, W., Jin, L., Du, Y., 2019. Adsorption properties of modified soda lime for carbon dioxide removal within the closed environment of a coal mine refuge chamber (vol 55, pg 10794, 2016). Ind Eng Chem Res. 58, 15379-15379. https://doi.org/10.1021/acs.iecr.9b03826.

Gao, N., Jin, L., Hu, H., Huang, X., Zhou, L., Fan, L., 2015. Potassium superoxide oxygen generation rate and carbon dioxide absorption rate in coal mine refuge chambers. Int J Min Sci Techno. 25, 151-155. https://doi.org/10.1016/j.ijmst.2014.12.001.

Gao, X., Yuan, Y., Cao, X., Wu, H., Zhao, X., 2017. Coupled cooling method and application of latent heat thermal energy storage combined with pre-cooling of envelope: Sensitivity analysis and optimization. Process Saf Environ. 107, 438-453. https://doi.org/10.1016/j.psep.2017.03.005.

Gao, X., Yuan, Y., Cao, X., Wu, H., Zhao, X., Yan, D., 2018. Coupled cooling method and application of latent heat thermal energy storage combined with pre-cooling of envelope: Temperature control using phase-change chair. Sustain Cities Soc. 42, 38-51. https://doi.org/10.1016/j.scs.2018.06.032.

Gao, X., Yuan, Y., Wu, H., Cao, X., Zhao, X., 2018. Coupled cooling method and application of latent heat thermal energy storage combined with pre-cooling of envelope: Optimization of pre-cooling with intermittent mode. Sustain Cities Soc. 38, 370-381. https://doi.org/10.1016/j.scs.2018.01.014.

Gao, X., Zhang, Z., Xiao, Y., 2020. Modelling and thermo-hygrometric performance study of an underground chamber with a long vertical earth-air heat exchanger system. Appl Therm Eng. 180, https://doi.org/10.1016/j.applthermaleng.2020.115773.

Halim, A., Brune, J., 2019. Do refuge chambers represent a good strategy to manage emergencies in underground coal mines? Mining Metal Explor. 36, 1191-1199. https://doi.org/10.1007/s42461-019-0100-8.

Hao, X., Guo, C., Lin, Y., Wang, H., Liu ,H., 2016. Analysis of heat stress and indoor climate control requirements for movable refuge chambers. Int J Environ Res Public Health. 13, 518-527. https://doi.org/10.3390/ijerph13050518.

Hirata, A., Nomura, T., Laakso, I., 2015. Computational estimation of body temperature and sweating in the aged during passive heat exposure. Int J Therm Sci. 89, 154-163. https://doi.org/10.1016/j.ijthermalsci.2014.11.001.

Jia, Y., Liu, Y., Liu, W., Li, Z., 2014. Study on purification characteristic of CO_2 and CO within closed environment of coal mine refuge chamber. Sep Purif Technol, 130: 65-73. https://doi.org/10.1016/j.seppur.2014.04.014.

Jia, Y., Liu, Y., Sun, S., Li, H., Jiao, L., 2015. Refrigerating characteristics of ice storage capsule for temperature control of coal mine refuge chamber. Appl Therm Eng. 75, 756-762.

https://doi.org/10.1016/j.applthermaleng.2014.10.036.
Kajtár, L., Herczeg, L., 2012. Influence of carbon-dioxide concentration on human well-being and intensity of mental work. Idojaras (Budapest, 1905). 116, 145-169. https://www.researchgate.net/publication/231558578.
Klein, M., Yantek, D., Hepokoski, M., Yan, L., 2017. Prediction of human core temperature rise and moisture loss in refuge alternatives for underground coal mines. Trans Soc Min Metall Explor Inc. 342, 29-35. https://doi.org/10.19150/trans.8105.
Lee, K., Spath, N., Miller, M., Mills, N., Shah, A., 2020. Short-term exposure to carbon monoxide and myocardial infarction: A systematic review and meta-analysis. Environ Int. 143, 105901. https://doi.org/10.1016/j.envint.2020.105901.
Li, F., Jin, L., Han, H., Huang, Z., Zhang, N., 2013. Volume of pressurized air and real experiment of mine refuge stations. Journal of Liaoning Technical University (Natural Science). 32, 55-58. (In Chinese)
Li, Y., Yuan, Y., Li, C., Han, X., Zhang, X., 2018. Human responses to high air temperature, relative humidity and carbon dioxide concentration in underground refuge chamber. Build Environ. 131, 53-62. https://doi.org/10.1016/j.buildenv.2017.12.038.
Luo, M., Wang, Z., Ke, K., Cao, B., Zhai, Y., Zhou, X., 2018. Human metabolic rate and thermal comfort in buildings: the problem and challenge. Build Environ. 131, 44-52. https://doi.org/10.1016/j.buildenv.2018.01.005.
Mejias, C., Jimenez, D., Munoz, A., Reyes-Bozo, L., 2014. Clinical response of 20 people in a mining refuge: Study and analysis of functional parameters. Safety Sci. 63, 204-210. https://doi.org/10.1016/j.ssci.2013.11.011.
Moreno, H., Pontiga, F., Valverde, J., 2021. Low concentration CO_2 capture in fluidized beds of $Ca(OH)_2$ as affected by storage humidity. Chem Eng J. 407, 127179. https://doi.org/10.1016/j.cej.2020.127179.
Nitter, T., Grande, M., Svendsen, K., Jørgensen, R., Carlucci, S., Cao, G., 2020. Can CO_2 sensors in the ventilation system of a pool facility help reduce the variability in the trihalomethane concentration observed in indoor air? Environ Int. 138, 105665. https://doi.org/10.1016/j.envint.2020.105665.
Onifade, M., 2021. Towards an emergency preparedness for self-rescue from underground coal mines. Process Saf Environ. 149, 946-957. https://doi.org/10.1016/j.psep.2021.03.049.
Paul, M., Iryanto, D., Quinn, D., Widyastutie, A., Mone A., 2019. Design and construction of high capacity fixed refuge chambers at PT freeport Indonesia's underground operations. Proceedings of the 11th International Mine Ventilation Congress. Springer, Singapore. https://doi.org/10.1007/978-981-13-1420-9_73.
Shao, H., Jiang, S., Tao, W., Wu, Z., Zhang, W., Wang, K., 2016. Theoretical and numerical simulation of critical gas supply of refuge chamber. International journal of mining science and technology. 26, 389-393. https://doi.org/10.1016/j.ijmst.2016.02.004
Shi, X., Zhu, N., Zheng, G., 2013. The combined effect of temperature, relative humidity and work intensity on human strain in hot and humid environments. Build. Environ. 69, 72-80. https://doi.org/10.1016/j.buildenv.2013.07.016.
Shimazaki, Y., Katsuta, S., 2019. Spatiotemporal sweat evaporation and evaporative cooling in thermal environments determined from wearable sensors. Appl Therm Eng. 163, https://doi.org/10.1016/j.applthermaleng.2019.114422.
Shu, W., Jin, L., Han, Z., Li, Y., Ou, S., Na, G., Huang, Z., 2017. Discharging performance of a forced-circulation ice thermal storage system for a permanent refuge chamber in an underground mine. Appl Therm Eng. 110, 703-709. https://doi.org/10.1016/j.applthermaleng.2016.08.192.
Sun, Z., Fang, W., Zhao, L., Chen, H., He, X., Li, W., Tian, P., Huang, Z., 2019. g-C_3N_4 foam/Cu_2O QDs with excellent CO_2 adsorption and synergistic catalytic effect for photocatalytic CO_2 reduction. Environ Int. 130, https://doi.org/10.1016/j.envint.2019.06.008.
Trackemas, J., Thimons, E., Bauer, E., Sapko, M., Zipf Jr. R., Schall, J., Rubinstein E., Finfinger G., Patts L.,

LaBranche N., 2015. Facilitating the use of built-in-place refuge alternatives in mines. USA, DHHS (NIOSH) publication No RI9698, Pittsburgh, PA. https://www.cdc.gov/niosh/mining/UserFiles/works/pdfs/2015-114.pdf.

Wu, B., Lei, B., Zhou, C., Zhao. Z., 2012. Experimental study of phase change material's application in refuge chamber of coal mine. Procedia engineering. 45, 936-941. https://doi.org/10.1016/j.proeng.2012.08.262.

Wu, Q., Liu, J., Zhang, L., Zhang, J., Jiang, L., 2020. Effect of temperature and clothing thermal resistance on human sweat at low activity levels. Build Environ. 183, 107117. https://doi.org/10.1016/j.buildenv.2020.107117.

Xu, X., You, S., Zheng, X, Zhang, H., Liu, S., 2017. Cooling performance of encapsulated ice plates used for the underground refuge chamber. Appl Therm Eng. 112, 259-272. https://doi.org/10.1016/j.applthermaleng.2016.10.072.

Yan, L., Yantek, D., Reyes, M., 2020a. Underground Mine Air and Strata Temperature Change Due to the Use of Refuge Alternatives. Mining Metall Explor. 37, 773-781. https://doi.org/10.1007/s42461-019-00153-0.

Yan, L., Yantek, D., Reyes, M., Whisner, B., Bickson, J., Srednicki, J., Damiano, N., Bauer, E., 2020b. Cryogenic air supply for cooling built-in-place refuge alternatives in hot mine. Mining Metall Explor. 37, 861-871. https://doi.org/10.1007/s42461-020-00194-w.

Yan, L., Yantek, D., Lutz, T., Yonkey, J., Srednicki, J., 2017. Heat mitigation for underground coal mine refuge alternatives using cryogenic air or borehole air supplies external. ASME 2017 International Mechanical Engineering Congress and Exposition, November, 2017, Tampa, Florida. https://doi.org/10.1115/IMECE2017-70432.

Yang, J., Yang, L., Wei, J., Ma, Y., Zhang, Z., 2013. Study on open-cycle carbon dioxide refrigerator for movable mine refuge chamber. Appl Therm Eng. 52, 304-312. https://doi.org/10.1016/j.applthermaleng.2012.12.014.

Yang, L., Wang, X., Li, M., Zhou, X., Liu, S., Zhang, H., Arens, E., Zhai, Y., 2020. Carbon dioxide generation rates of different age and gender under various activity levels. Build Environ. 186, 107317. https://doi.org/10.1016/j.buildenv.2020.107317.

Yantek, D., Yan, L., Damiano, N., Reyes, M., Srednicki, J., 2019. A test method for evaluating the thermal environment of underground coal mine refuge alternatives. Int J Min Sci Techno. 29, 343-355. https://doi.org/10.1016/j.ijmst.2019.01.004.

Yuan, Y., Gao, X., Wu, H., Zhang, Z., Cao, X., Sun, L., Yu, N., 2017. Coupled cooling method and application of latent heat thermal energy storage combined with pre-cooling of envelope: Method and model development. Energy. 119, 817-833. https://doi.org/10.1016/j.energy.2018.06.151.

Zhai, Y., Li, M., Gao, S., Yang, L., Zhang, H., Arens, E., Gao, Y., 2018. Indirect calorimetry on the metabolic rate of sitting, standing and walking office activities. Build Environ. 145, 77-84. https://doi.org/10.1016/j.buildenv.2018.09.011.

Zhang, Q., Lu, W., Wu, M., Qi, G., 2021. Application of amine-modified porous materials for CO_2 adsorption in mine confined spaces. Colloid Surface A. 629, 127483. https://doi.org/10.1016/j.colsurfa.2021.127483.

Zhang, X., Wargocki, P., Lian, Z., 2016. Human responses to carbon dioxide, a follow-up study at recommended exposure limits in non-industrial environments. Build Environ. 100, 162-171. https://doi.org/10.1016/j.buildenv.2016.02.014.

Zhang, Z., Day, R., Wang, K., Wu, H., Yuan, Y., 2018. Thermal performance analysis of an underground closed chamber with human body heat sources under natural convection. Appl Therm Eng. 145, 453-463. https://doi.org/10.1016/j.applthermaleng.2018.09.068.

Zhang, Z., Wu, H., Wang, K., Day, R., Yuan, Y., 2019. Thermal performance of a mine refuge chamber with human body heat sources under ventilation. Appl Therm Eng. 162, https://doi.org/10.1016/j.applthermaleng.2019.114243.

Zhang, Z., Wu, H., Wang, K., Day, R., Yuan, Y., 2020. Air quality control in mine refuge chamber with ventilation through pressure air pipeline. Process Saf Environ. 135, 46-58. https://doi.org/10.1016/j.psep.2019.12.014.

Zhang, Z., Yuan, Y., Wang, K., 2017. Effects of number and layout of air purification devices in mine refuge chamber. Process Saf Environ. 105, 338-347. https://doi.org/10.1016/j.psep.2016.11.023.

Zhu, S., Jenkins, S., Addo, K., Heidarinejad, M., Romo, S., Layne, A., Ehizibolo, J., Dalgo, D., Mattise, N., Hong, F., Adenaiye, O., de Mesquita, J., Albert, B., Washington-Lewis, R., German, J., Tai, S., Youssefi, S., Milton, D., Srebric, J., 2020. Ventilation and laboratory confirmed acute respiratory infection (ARI) rates in college residence halls in College Park, Maryland. Environ Int. 137, https://doi.org/10.1016/j.envint.2020.105537.

Wolkoff, P., Kjærgaard, S., 2007. The dichotomy of relative humidity on indoor air quality. Environ Int. 33, 850-857. https://doi.org/10.1016/j.envint.2007.04.004.